



Phase Transfer Catalyst Stabilized Metal Nanoparticles for Free Radical Polymerization

Egambaram Murugan¹, *A. Rubavathy Jaya Priya¹ and P. Amirthalingam²

¹Department of Physical chemistry, School of Chemical sciences, University of Madras, Guindy, Chennai-600 025, Tamil Nadu, INDIA

²Department of Physics, Periyar University, Salem, Tamil Nadu, INDIA

(Received 08th September 2014, Accepted 30th November 2014)

Abstract: A new catalytic approach in the free radical polymerization reaction of acrylonitrile (AN) using $K_2S_2O_8$ as a water soluble initiator in biphasic medium was established using cetyltrimethylammonium bromide (CTAB) as conventional PTC and MNPTC's. The three types of homogeneous metal nanoparticle catalyst (MNPTC) viz., CTAB-RuNpsC, CTAB-AuNpsC and CTAB-AgNpsC were synthesized using CTAB as a common stabilizing agent and respective metal salts as their precursors. The formations of these metal nanoparticles irrespective of the metal catalysts were confirmed with FT-IR, UV-VIS and TEM techniques. The kinetic study of the polymerization reaction using CTAB as PTC was carried out initially to find the steady state rate of polymerization and the order of the reaction. After fixing the steady state rate as 50 mins and other parameters like concentration of monomer, initiator and temperature as constant, the comparative catalytic activities of the catalyst were examined. From the observed rate of polymerization (R_p) the order of activity of catalyst were determined as CTAB-RuNpsC > CTAB-AuNpsC > CTAB-AgNpsC >> CTAB. Further, the image of the acrylonitrile polymer formed from the CTAB-RuNpsC catalyst was studied using FESEM microscope. On the basis of the obtained results, a mechanism is proposed for the polymerization reaction.

Keywords: Nano-phase transfer catalyst, surfactant, cetyltrimethylammonium bromide, metal nanoparticles and free radical polymerization.

© 2014 IJRCE. All rights reserved

Introduction

The phase transfer catalyst (PTC) has been considered as a potent and versatile synthetic tool due to its simplicity and low cost not only in organic chemistry^[1] but also in inorganic chemistry, analytical application, electrochemistry, photochemistry and polymer chemistry and the method has found universal adoption^[2,3,4]. The interest in PTC aided free radical polymerization of vinyl monomers such as butyl acrylate, acrylonitrile (AN), methyl methacrylate^[5], glycidyl methacrylate, butyl methacrylate and methacrylate^[6] using water-soluble initiators such as 2, 2' Azobisisobutronitrile (AIBN)^[7], peroxydisulphates (PDS)^[7] and peroxymonosulphates (PMS)^[5] in combination with suitable reducing agents producing free radicals, viz, $SO_4^{\bullet-}$, Cl^{\bullet} ^[8,9,10] and OH^{\bullet} responsible for initiation of polymerization has been continuously increased. Currently, the catalyst such as crown ethers^[11] or quaternary ammonium salts (QX) such as tetrabutylammonium bromide (TBAB)^[12] tetrabutylammonium hypochlorite ion^[8, 14] as phase transfer agents was an essential one. But incorporating the nanotechnological ideas into this field is an innovative idea that brings up a new chemistry to enlighten this specific area.

Contemplating this idea, in the recent past, the

research on nanoparticle science and engineering is mainly devoted to the fabrication of advanced integrated functionalized materials with nanoparticles for different applications^[15-17]. Metal nanoparticles have an ideal size which is responsible for the building blocks in the field of nanotechnology and are of great importance because they exhibit unique electronic, optic, photonic and catalytic properties^[18-22]. They may be composed of any substance including metals, semiconductors, core-shell composite architectures and organic polymers. The unique catalytic properties of nanosized materials should be acknowledged by differing it from the bulk material^[23,24]. In particular, these metal nanoparticles are playing a vital role in the preparation of homogenous and heterogeneous catalysts because of its effective utilization including the expensive transition metal field of catalysis^[25-28]. Especially, preparation of metal nanoparticle catalysts using gold,^[29-35] silver^[36-40] and ruthenium^[41,42] have been studied very often with different matrices because of their easy preparation, good stability and some interesting properties. Similarly, the preparations of nanoparticles with controlled size and shape through wet chemistry process have also been largely exploited^[33,43]. The reduction of these metals was normally carried out using reducing agent like sodium borohydride with structure directing stabilizing agent viz., surfactants eg.

CTAB^[44-51], SDS⁵², tetraoctylammonium bromide (TOAB)^[53], trisodium citrate (TSC)^[54], polymer supported matrices^[55], thiol groups^[56], etc. In the present study, we are focusing the preparation of 3 types of homogenous metal nanoparticle catalysts using CTAB as a common stabilizing agent and RuCl₃, HAuCl₄ and AgNO₃ as metal cursors which is the simplest and efficient way of synthesis.

However, to bridge these ideas, the PTC technique was rejuvenated by introducing the nanocatalyst (MNPTC) in the place of conventional one (PTC). Further, this study is also described the catalytic activity of metal nanoparticles in free radical polymerization (FRP) of AN and their mechanism in detail.

Material and Methods

The chemicals such as acrylonitrile (AN, s-d chem), auric chloride (HAuCl₄.3H₂O, Sigma Aldrich), Cetyltrimethyl ammonium bromide (CTAB, SD fine), ruthenium(III) chloride hydrate (RuCl₃.nH₂O, Loba), silver nitrate (AgNO₃) and sodium borohydride (SBH, Sigma Aldrich) were used as such without further purification. Benzene, ethanol, methanol were purified by the procedure as described in the literature. Potassium peroxydisulphate (PDS) was purified by crystallisation

thrice by water. Deionised water obtained by multiple distillations was used for the preparation of the solutions.

Preparation of CTAB stabilized metal nanoparticles (CTAB-MNpsC): Three different 50 ml round bottom (RB) flask were taken individually in which 5 ml of stabilizing agent viz., CTAB (5×10^{-3} M) was added in each vials and allowed to dissolve in double distilled (DD) water under stirring for about half an hour^[57]. Simultaneously, the three different types of metal precursor solution viz., RuCl₃, HAuCl₄ and AgNO₃ were prepared for about 5 ml by fixing the concentration as 5×10^{-3} M using DD water and added individually to the RB flask containing CTAB solution. Then the respective CTAB metal nanoparticle solution mixtures were stirred individually for about half an hour. To this solution 0.6 ml (1×10^{-2} M) of ice-cold aq. SBH was added in aliquots to the each mixture under stirring and was continued until the respective metal gets reduced into zerovalent states as shown in Scheme.2.1. The appearance of the dark green from dark brown colour, gold forms purple red from yellow colour and light orange from colourless was noticed for CTAB stabilized ruthenium nanoparticles (CTAB-RuNpsC), CTAB stabilized gold nanoparticles (CTAB-AuNpsC) and CTAB stabilized silver nanoparticles (CTAB-AgNpsC) respectively as shown in Figure 3.1 confirms visually the formation of ruthenium nanoparticles, gold nanoparticles and silver nanoparticles.

Scheme 2.1. Preparation of 3 types of CTAB stabilized metal nanoparticle catalysts

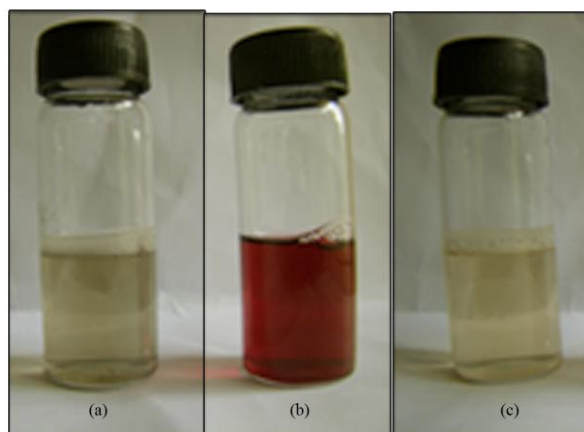


Figure 3.1: Photograph of the CTAB-RuNpsC (a), CTAB-AuNpsC (b) and CTAB-AgNpsC (c) nanoparticles solution

Thus the prepared three types of homogenous nanoparticle solutions viz., CTAB-RuNpsC, CTAB-AuNpsC and CTAB-AgNpsC were characterized individually with FT-IR, UV-VIS and TEM techniques. The observed FT-IR spectra for the CTAB and the lyophilized solutions of CTAB-RuNpsC, CTAB-AuNpsC and CTAB-AgNpsC were shown in Figure 3.2a, 3.2b, 3.2c & 3.2d respectively. Similarly the UV-VIS spectra for CTAB-RuNpsC, CTAB-AuNpsC and CTAB-AgNpsC solutions were presented in Figure 3.3a, 3.3b & 3.3c respectively. The microscopic images of CTAB stabilized metal nanoparticles were shown in Figure 3.4a (CTAB-RuNpsC), Figure 3.4b (CTAB-AuNpsC) and Figure 3.4c (CTAB-AgNpsC) were recorded from transmission electron microscope (TEM).

The CTAB-RuNpsC, CTAB-AuNpsC and CTAB-AgNpsC nanoparticles thus formed and confirmed using the above techniques were used as the nano-phase transfer catalyst (MNPTC) viz in the free radical polymerization. The image of the polymer acrylonitrile formed from CTAB-RuNpsC were recorded using field emission scanning electron microscope (FESEM) were shown in Figure 3.5a & 3.5b.

Free radical polymerization (FRP) of AN using all the homogenous metal nanoparticle catalyst: The polymerization reaction was conducted in a thermostatic water bath of 20 litre capacity using the polymerization reaction tube made up of pyrex glass with 100 ml capacity having B24 quick fit socket fitted with B24 cone provision of inlet and outlet for argon gas. This water bath is equipped with an electrical fitter and a mechanical stirrer to maintain the constant temperature with an accuracy of $60 \pm 0.1^\circ\text{C}$. The PTC viz., CTAB were used initially by fixing the concentration as $2 \times 10^{-2} \text{ M}$ for free radical polymerization of AN with $\text{K}_2\text{S}_2\text{O}_8$ as a initiator under unstirred condition. The common procedure for polymerization reactions was conducted by taking equal volumes of aqueous phase (10 ml) and organic phase (10 ml). That is, irrespective of catalyst solution, 10 ml of aqueous phase containing 1ml ($2 \times 10^{-3} \text{ M}$) of catalyst solution and 9 ml of initiator solution and 10 ml of organic phase (monomer (1 ml) + benzene (9 ml)) was taken individually in polymerization tube and then the dissolved oxygen in the reaction mixture has been expelled by passing the argon gas and subsequently and the reaction tube was placed in thermostat maintained at $60 \pm 0.1^\circ\text{C}$. The addition of initiator solution has been treated as a zero time (starting time) of the reaction. After the specific reaction time was over the polymerization was arrested by pouring the solution into the ice cold excess methanol and then after repeated washing the unreacted monomer has been removed and thus the obtained polymer present in the cintered crucible was weighed to determine the amount of polymer formed.

From the polymer yield, the rate of polymerization R_p was evaluated by using the following equation,

$$R_p = 1000.W / V.t.M \quad \text{Eqn. 1}$$

Where, W= weight of the polymer obtained (gm), V= Volume of reaction mixture (ml), t= reaction time (sec) and M= molecular weight of monomer (gm)

Based on the obtained polymer weight, the yield of the polymer was calculated using the Eqn.1, and the R_p of the each catalyst was determined as given in Table. 2. The steady state rate of the polymerization of AN was evaluated by plotting R_p vs time for the PTC viz., CTAB ($2 \times 10^{-2} \text{ M}$) initiated by $\text{K}_2\text{S}_2\text{O}_8$ in a benzene/water biphasic at 60°C . Fixing this as the steady state rate of polymerization, the three different MNPTC such as CTAB-RuNpsC, CTAB-AuNpsC and CTAB-AgNpsC as catalyst were used individually by fixing $2 \times 10^{-3} \text{ M}$ concentration for free radical polymerization of AN with $\text{K}_2\text{S}_2\text{O}_8$ as a initiator under unstirred condition.

Results and Discussion

Preparation of homogeneous nanoparticle catalyst using amphiphilic surfactant as a template is an attractive area of current interest. Especially, free radical polymerization using nanoparticle phase transfer catalyst instead of conventional catalyst has proved to be an efficient one. Hence, in this study, we have prepared 3 different of type homogeneous nanoparticle solutions such as CTAB-RuNpsC, CTAB-AuNpsC and CTAB-AgNpsC as a common template/stabilizing agent and the respective metal salt as a metal precursor.

Visual analysis

In the preparation of catalyst, soon after the addition of sodium borohydride to each solution, a characteristic colour change was observed irrespective of homogenous nanoparticle catalyst. That is, ruthenium gave dark green from dark brown colour, gold forms purple red from yellow colour and silver gave light orange colour from colourless as shown in the Figure 3.1. The colour changes noticed in each catalyst solution as an indication for the formation of respective metal nanoparticle catalyst. In order to confine this observation further, these catalysts were once again examined by different analytical techniques.

Spectroscopic and microscopic analysis

FT-IR (ATR) Spectroscopy:

The binding of the metal nanoparticles with the ammonium ions of the CTAB established through their M-N stretching irrespective of the metal catalyst. That is, the peak noticed at 2288 cm^{-1} -C-N⁺(CH₃)₃ Figure 3.2a in CTAB (control) was shifted to 2143 cm^{-1} in the FT-IR spectra of CTAB-RuNpsC (Figure 3.2b), 2135 cm^{-1} for CTAB-AuNpsC (Figure 3.2c) and 2131 cm^{-1} for CTAB-AgNpsC (Figure 3.2d) catalysts and this observation confirms the stabilization of the metal nanoparticles with CTAB. Similarly the presence of alkyl chain irrespective of catalyst was confirmed through the characteristic peak noticed at 1480 cm^{-1} for CH₂ and CH₃ stretching. Further the C-N stretch shift from 1244 cm^{-1} (CTAB) to 1219 cm^{-1} (CTAB-RuNpsC), 1220 cm^{-1} (CTAB-AuNpsC) and 1220.13 cm^{-1} (CTAB-RuNpsC) confirms that the metal nanoparticle has been attached to the Nitrogen by vanderwalls attraction.

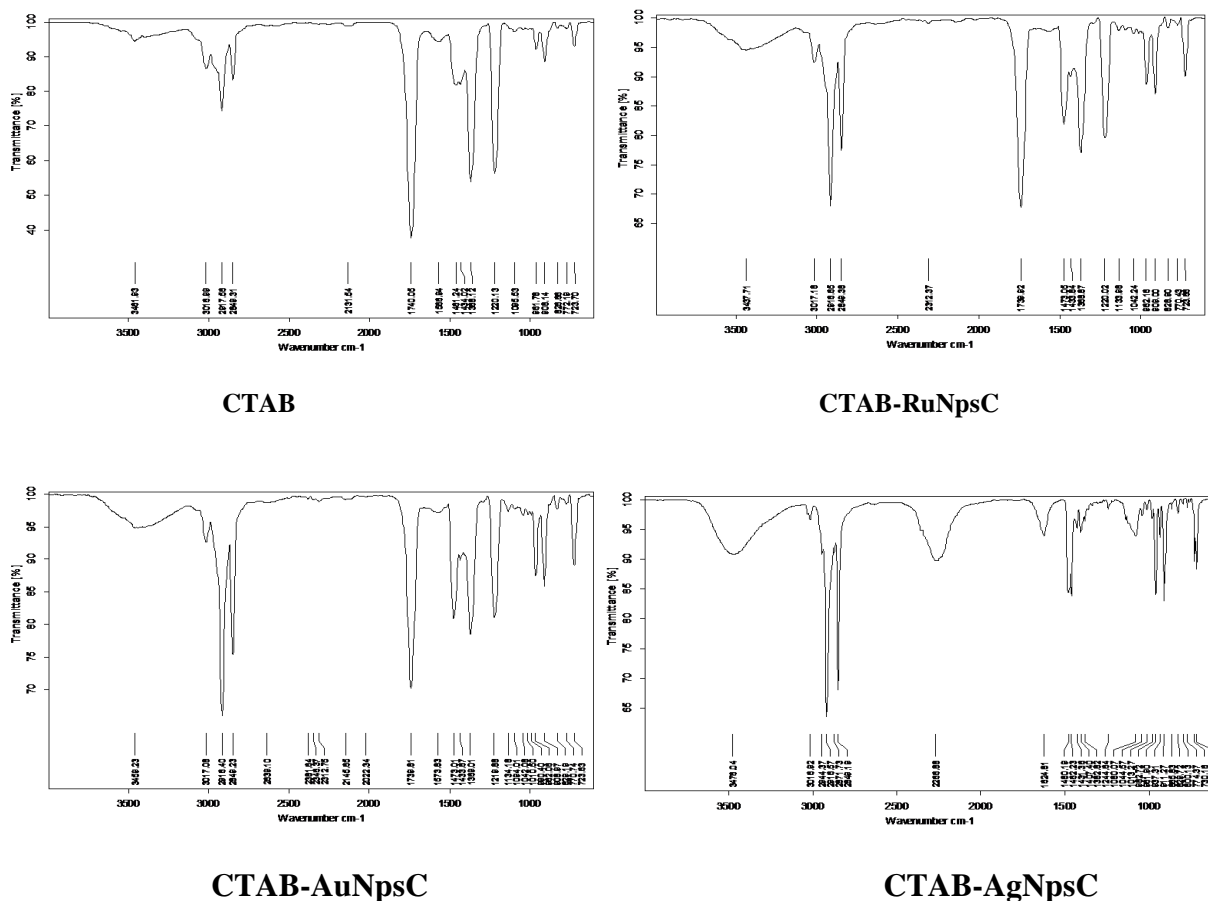


Figure 3.2: FT-IR (ATR) Spectrum of CTAB and CTAB stabilized metal nanoparticles

Table 3.1
Stretching frequency values of the CTAB & CTAB stabilized metal nanoparticles obtained using the FT-IR (ATR) spectroscopy

Sample Name	CTAB	CTAB-RuNpsC	CTAB-AuNpsC	CTAB-AgNpsC
(N-H) stretching	3478	3437	3459	3481
(N ⁺ - CH ₃ C-H) stretching	3018	3017	3017	3018
(CH ₂) stretching	2918	2918	2918	2917
(CH ₂) stretching	2849	2849	2849	284
(N ⁺ - CH ₃) headgroup methylene vibrations	1480	1473	1473	1481
(N ⁺ - CH ₃) headgroup methylene vibrations	1431	1433	1433	1434
(C-N ⁺) stretching	1044	1042	1042	
(C-N ⁺) stretching	951	952	952	951
(C-N ⁺) stretching	911	909	908	908

The detailed stretching frequency of the CTAB (control) and CTAB stabilized metal nanoparticles are exhibited in the Table. 3.1.

UV-VIS Spectroscopy: The UV-VIS study explores the possibility of extending the absorption to the visible region for a band at 392 nm (Figure 3.3a), which disappears when all of the Ru³⁺ are completely reduced to Ru⁰ in CTAB-RuNpsC and similar observations has already been reported [58,59]. This absorption spectroscopy has also been used to infer the particle size for CdS

colloids in the size regime where the absorption spectrum is dependent on the particle size eg: 2-4 nm. Similarly, in our study also, the UV spectrum of CTAB-AuNpsC (Figure 3.3b) has shown a red shift in the surface Plasmon band at 525 nm along with several blue band and these values clearly proves that the Au was exist in nanosize and the size of the AuNps particle are smaller [61,62]. Similar observation has already been noticed. In the case of CTAB-AgNpsC, a broad band was noticed at 413 nm (Figure 3.3c) thus confirmed the formation of AgNps and this observation agrees well with the earlier studies

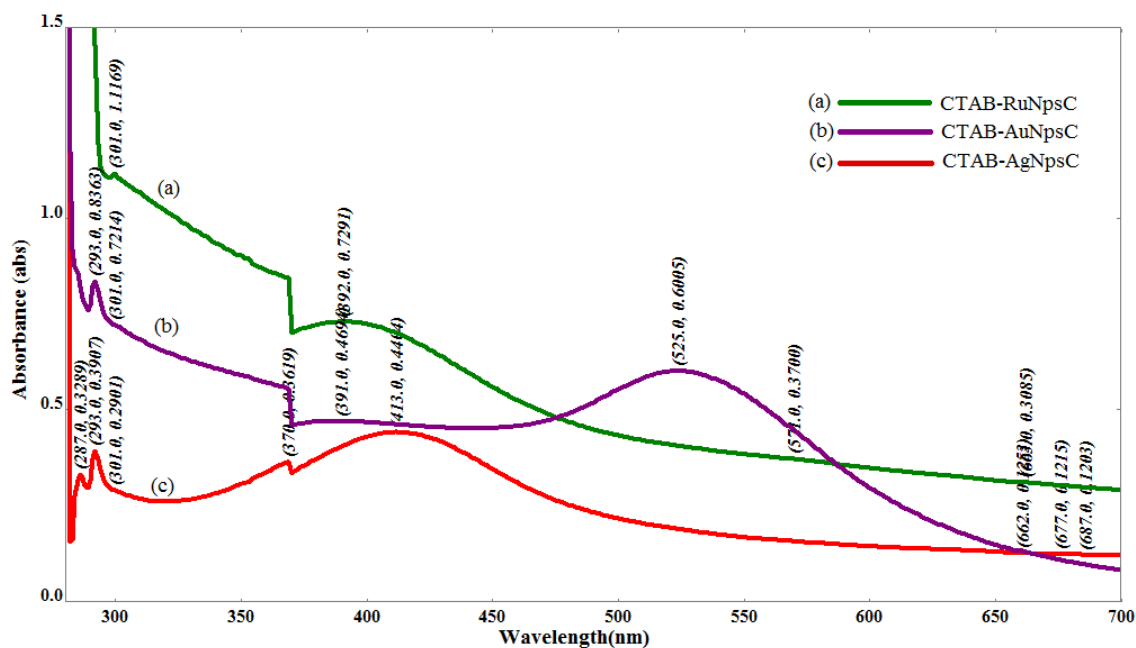


Figure 3.3: UV-VIS spectrum of CTAB stabilized metal nanoparticle solutions

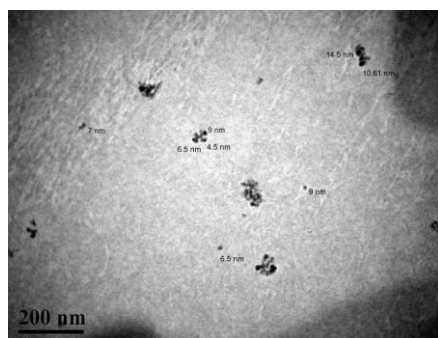


Figure 3.4a: TEM image of CTAB stabilized ruthenium nanoparticle solution (CTAB-RuNpsC)

size, smooth surface and large surface area-to-volume ratio are established.

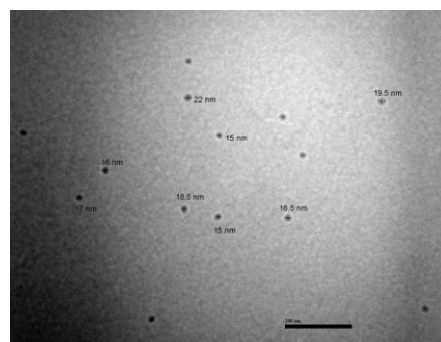


Figure 3.4c: TEM image of CTAB stabilized silver nanoparticle solution (CTAB-AgNpsC)

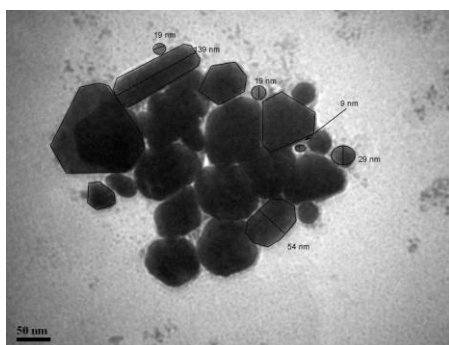


Figure 3.4b: TEM image of CTAB stabilized gold nanoparticle solution (CTAB-AuNpsC)

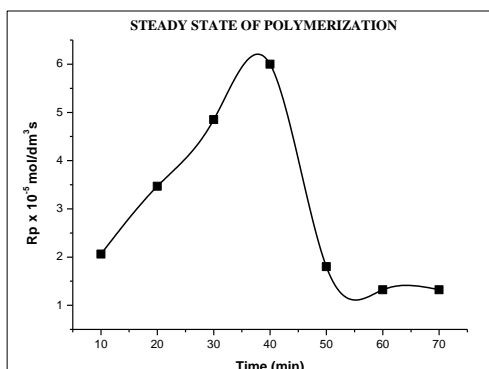
Transmission Electron Microscope (TEM): In order to confirm the formation of the nanoparticles using TEM, the sample preparation was carried out by dropping the solution on the carbon coated copper grid and allowed to dry in air. Generally, from the microscopic technique, the selection of the best nanoparticle catalysts having smaller

The images are taken from the respective samples after a year ago, even though we took the image after a long time we noticed that they showed a no alteration in ruthenium nanoparticles and silver nanoparticles while growth in size from 9 nm to 139 nm and above in the case of gold nanoparticles^{69,70}. The image of CTAB-RuNpsC (Figure 3.4a) depicts the closely arranged nanoparticle which is smaller 5 nm and above in size. Similarly in the case of CTAB-AuNpsC (Figure 3c) the image shows the formation of nanosphere is measured to have 9 nm and above. There are larger size of nanoparticles found in this image is because for the formation of the nanoshapes such as nanotriangle, nanorods from the nanosphere^[71-73] which is the feature of the shape gold nanoparticles and also to verify that even after one year they did not aggregate either they grew larger in size. In the case of CTAB-AgNpsC (Figure 3d) the formation of nanospheres with larger in

size 15 nm and above on [52, 63-68] compared with CTAB-RuNpsC and CTAB-AuNpsC were noticed and these observation shows that the size of the nanoparticles in CTAB colloids may be smaller in CTAB-RuNpsC, little higher in CTAB-AuNpsC and still bigger size in CTAB-AgNpsC.

Free Radical Polymerization of AN

The polymerization of AN initiated by K₂S₂O₈ using both the commercial catalyst viz., PTC (CTAB) and nano-phase transfer catalyst MNPTC (CTAB-RuNpsC, CTAB-AuNpsC and CTAB-AgNpsC) were carried out in benzene-water two phase systems under nitrogen atmosphere under unstirred conditions at 60°C. Initially, the control reaction was carried out using the CTAB as the catalyst under the identical conditions for fixing the steady state rate of polymerization to carry out the reaction using the MNPTC. Moreover, from the reaction catalysed using MNPTC, the mechanism of the polymerization reaction involved is established.



Steady-state Rp

Figure 3.5: Graph showing the steady state rate of polymerization of AN using CTAB as catalyst

The rate of polymerization (Rp) was calculated for every 10 mins for CTAB and the graph was obtained by plotting Rp versus time for about 70 mins. The initial value among the constant value from the graph is set as the steady-state Rp value of AN and was obtained at 50 min (Figure 3.5).

This value is set as the steady state rate of polymerization for all the MNPTC catalyst in the polymerization of AN irrespective of the catalyst.

Comparative catalytic efficacy: The most important factor here needs to be highlighted is the concentration of the metal nanoparticle catalyst. That is, we employed exactly 10 fold lesser concentration (2 x 10⁻³M) irrespective of the CTAB-RuNpsC, CTAB-AuNpsC and CTAB-AgNpsC than with the plain CTAB concentration i.e., 2 x 10⁻²M. The Rp observed in all nanoparticle catalysts was found to be enhanced to ≈ 8 fold than with the plain PTC's as shown in the Table. 3.2. This is because of the active acceleration of the respective metal nanoparticles viz., the small size and large surface of the nano-phase transfer catalyst makes the polymer to have more yields compare to the bulk material (CTAB) as

To confirm this the formation of the polymer was studied by observing the image.

Table 3.2

Rate of polymerization of AN at steady state rate of polymerization using CTAB-RuNpsC, CTAB-AuNpsC and CTAB-AgNpsC catalyst

Rate of Polymerization Rp x 10 ⁵ mol dm ⁻³ s ⁻¹	
CTAB-RuNpsC	8.3
CTAB-AuNpsC	7.98
CTAB-AgNpsC	7.75

Field Emission Transmission Electron Microscope (FESEM) of an polymer:

The AN polymer formed from the catalyst CTAB-RuNpsC was alone taken for its surface and reactivity study. The FESEM image shown in Figure shows the initiation step of the polymer as small nanorods being formed on the surface of the already formed polymer flakes. From the image as in Figure 3 it is observed in another place of the same polymer, the two pieces of the polymer are being formed on the surface of the polymer from small nanorods to a bigger flake.

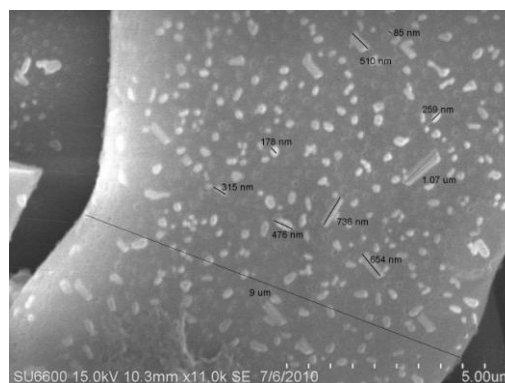


Figure 3.5a: FESEM image of polymer AN formed using the CTAB-RuNpsC catalyst

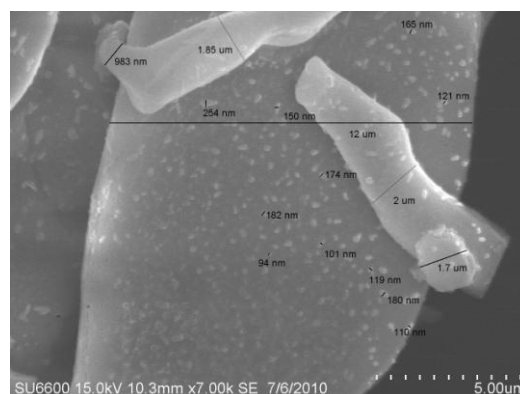
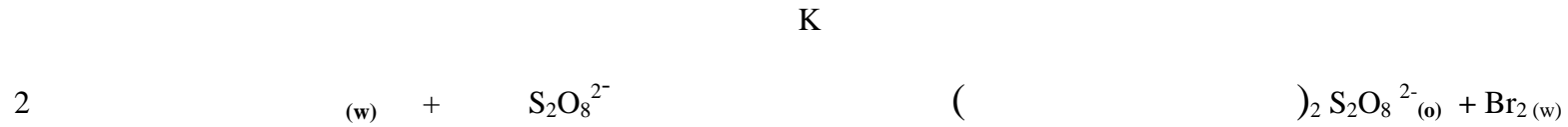


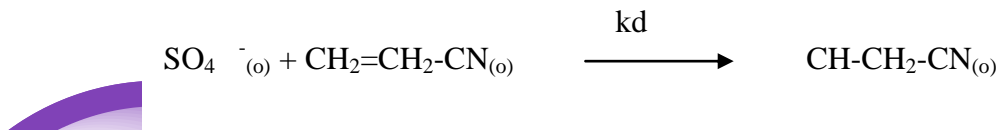
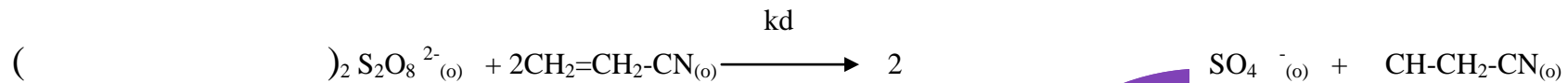
Figure 3.5b :FESEM image of polymer AN formed using the CTAB-RuNpsC catalyst

Mechanism for the polymerization of AN using MNPTC initiated by $K_2S_2O_8$ in benzene/water system:

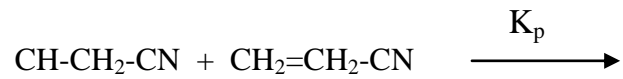
1) PHASE TRANSFER OF NANO MNPTC



2) INITIATION



3) PROPOGATION



4) TERMINATION



Conclusion

We have clearly demonstrated the synthesis of 3 different homogenous nanoparticles catalyst viz., CTAB-RuNpsC, CTAB-AuNpsC and CTAB-AgNpsC and were characterized using FT-IR, UV-VIS and TEM analyses. The observed spectroscopic and microscopic results proves the formation and stabilization of RuNps, AuNps and AgNps in CTAB and the images shows to have increasing order of size i.e., RuNps > AuNps > AgNps which is mainly an important fact responsible for the effective catalyst. In the synthesis of CTAB-MNpsC, the concentration of CTAB is below CMC i.e., 2×10^{-3} M in the nano-phase transfer catalyst such as CTAB-RuNpsC, CTAB-AuNpsC and CTAB-AgNpsC compare to the plain CTAB concentration to be 2×10^{-2} M. Even though the concentration is below CMC and less by 10 times than the control, the CTAB-MNpsC shows the catalytic activity found to increase by ≈ 8 fold in the polymerization of AN. From the analytical techniques and from the polymerization reaction it is obvious that CTAB-RuNpsC is the best catalyst compare to the other PTC stabilized metal nanoparticles in the free radical polymerization reaction of acrylonitrile.

References

- Sanjeev D. Naik and L. K. Doraiswamy, *AIChE Journal*, **44**(3), 612-646 (1998)
- Senthamizh Selvi R., Nanthini R. and Sukanyaa G., *Int. J. Sci. & Tech. Res.*, **1**(3), 61-63 (2012)
- Murugan E., Tamizharasu G., *J. Mol. Cat. A: Chemical*, **363-364**, 81-89 (2012)
- Lohse S.E. and Murphy C.J., *J. Am. Chem. Soc.*, **134**, 15607-15620 (2012)
- Sunitha T.G., Yoganand K.S., Umamaheswari G., Umapathy M.V., *Int. J. Chem. Res.*, **3**(2), 18-24 (2012)
- Hurduc N., Surpateanu G. and Bulacovshchi V., *Polym. Bull.*, **30**, 69 (1993)
- Jayakrishnan A., Shah D., *J. Polym. Sci. Polym. Chem. Ed.* **21**, 3201-3208 (1983)
- Do J.S. and Do Y.L., *Electrochem. Acta*, **39** (15), 2299-2309 (1994)
- Do J.S. and Do Y.L., *Electrochem. Acta*, **39** (15), 2311-2319 (1994)
- Do J.S. and Do Y.L., *Electrochem. Acta*, **39** (13), 2037-2044 (1994)
- Rasmussen J.K. and Smith H.K., *J. Am. Chem. Soc.*, **103**, 730-731 (1981)
- Kitamura T., Kobayashi S., and Taniguchi H., *J. Org. Chem.*, **49**, 4755-4760 (1984)
- Murugan E., Gopinath, P., *J. Mol. Cat. A: Chemical* **294** (1-2), 68-73 (2008)
- Murugan E., Gopinath P., *J. Mol. Cat. A: Chemical* **309** (1-2), 12-20
- Alivisatos A.P., *Science*, **271**(5251), 933-937 (1996)
- Andres R.P., Bielefeld J.D., Henderson J.I., Janes D.B., Kolagunta V.R., Kubiak C.R., Mahoney W.J., Osifchin R.G., *Science*, **273**(5282), 1690-1693 (1996)
- Alivisatos A.P., Johnson K.P., Peng X.G., Wilson T.E., Loweth C.J., Bruchez M.P., Jr, Schultz P.G., *Nature*, **382**, 609-611 (1996)
- Cui Y., Q. Wei, H. Park, C. M. Lieber, *Science* 293(5533), 1289-1292 (2001)
- Mostafa A. El-sayed, *Accounts of Chemical Research*, **34**(4), 257-264 (2001)
- Christy F. Landes, Stephan Link, Mona B. Mohamed, Babak Nikoobakht, and Mostafa A. El-Sayed, *Pure Appl. Chem.*, **74**(9), 1675-1692 (2002)
- Wyatt P. McConnell, James P. Novak, Louis C. Brousseau III, Ryan R. Fuierer, Robert C. Tenent, and Daniel L. Feldheim, *J. Phys. Chem. B*, **104**, 8925-8930 (2000)
- Karen Grieve, Paul Mulvaney, Franz Grieser, *Current Opinion in Colloid & Interface Science*, **5**, 168-172 (2000)
- Nedeljkovic J.M., *Trends Adv. Mater. Processes, Mater. Sci. Forum*, **352**, 79 (2000)
- Yang J., Lee J. Y. and Ying J. Y., *Chem. Soc. Rev.*, **40**, 1672-1696 (2011)
- Kr'alik M. and Biffis A., *J. Mol. Cat. A: Chemical* **177**, 113-138 (2001)
- Toshima N., Metal nanoparticles for catalysis. In: nanoscale materials, L. M. Liz-Marza'n and P.V. Kamat(Eds.), Kluwer Academic Publishers, Boston, 79 (2003)
- Frens G., *Nature, Phys. Sci.*, **241**(105), 20-22 (1973)
- Andres R.P., Bielefeld J.D., Henderson J.I., Janes D.B., Kolagunta V.R., Kubiak C.R., Mahoney W.J., Osifchin R.G., *Science*, **273**(5282), 1690-1693 (1996)
- Alivisatos A.P., Johnson K.P., Peng X.G., Wilson T.E., Loweth C.J., Bruchez M.P., Jr, Schultz P.G., *Nature*, **382**, 609-611 (1996)

30. Robenek, H., *Colloidal Gold: Principles, Methods and Applications* M. A. Hayat, ed., **1(1)**, Academic Press, Inc., New York, (1989)
31. Hodak J.H., Henglein A., and Hartland G.V., *J. Chem. Phys.*, **114**, 2760 (2001)
32. Uechi I. & Yamada S., *Anal Bioanal Chem*, **391**, 2411–2421 (2008)
33. Brown K. R. and Natan M. J., *Langmuir*, **14**, 726-728 (1998)
34. Bagwe R.P., Mishra B.K., Khilar K.C., *J. Disp. Sci. Technol.*, **20(6)**, 1569-1579 (1999)
35. Petit C., Lixon P., Pileni M.P., *J. Phys. Chem.*, **97**, 12974-12983 (1993)
36. Taleb A., Petit C., Pileni M.P., *Chem. Mater.*, **9**, 950-959 (1997)
37. Bagwe R.P. and Khilar K.C., *Langmuir*, **16**, 905-910 (2000)
38. Krutyakov Yu. A., Rukhlya E.G., Artemov A.V., Olenin A. Yu., Ivanov M.N., and Shelyakov O.V., *Nanotechnologies in Russia*, **3(11-12)**, 756-762 (2008)
39. Sulman E., Doluda V., Dzwigaj S., Marceau E., Kustov L., Tkachenk O., Bykov A., Matveeva V., Sulman M., Lakina N., *J. Mol. Cat. A: Chemical*, **278**, 112-119 (2007)
40. Baruwati B., Polshettiwar V., Varma R.S., *Tetrahedron Letters*, **50**, 1215-1218 (2009)
41. Xu X.J., Chow P.Y., and Gan L.M., *J. Nanoscience Nanotechnol.*, **2**, 61(2002)
42. Jana N. R., Gearheart L., and Murphy C. J., *Adv. Mater.*, **13(18)**, 1389-1393 (2001)
43. Hernawan B. Purwono, Wahyunngsih T.D., *International Journal of Engineering & Technology*, **12(1)** 1-4
44. Chen S., Yao H. and Kimura K., *Langmuir*, **17**, 733-739 (2001)
45. Brown K. R., Walter D. G., and Natan M. J., *Chem. Mater.*, **12**, 306-313 (2000)
46. Murphy C.J., Sau T. K., Gole A. M., Orendorff C. J., Gao J., Gou L., Hunyadi S.E., and T. Li, *J. Phys. Chem. B*, **109**, 13857-13870 (2005)
47. Rnblom M.T. and U. Henriksson, *J. Phys. Chem. B*, **101**, 6028-603 (1997)
48. Yu Y. Ying, S. Sing Chang, C. Liang Lee, and C. R. Chris Wang, *J. Phys. Chem. B*, **101(34)**, 6661-6664 (1997)
49. Brown K. R. and Natan M. J., *Langmuir*, **14**, 726-728 (1998)
50. Bagwe R. P. and Khilar K. C., *Langmuir*, **16**, 905-910 (2000)
51. Jana N.R., Gearheart L., Murphy C.J., *Chem. Commun.*, 617 (2001)
52. Brown K. R., Walter D. G., and Natan M. J., *Chem. Mater.*, **12**, 306-313 (2000)
53. Craig G.E., Brown S.D., Lamprou D. A., Graham D., and Wheate N.J., *Inorg. Chem.*, **51**, 3490–3497 (2012)
54. Chen S., Yao H. and Kimura K., *Langmuir*, **17**, 733-739 (2001)
55. Babak Nikoobakht and Mostafa A. El-Sayed, *Chem. Mater.*, **15**, 1957-1962 (2003)
56. Miyazaki A., Balint I., Aika K., Nakano Y., *J Catal*, **204**, 364–371 (2001)
57. Durap F., Zahmakiran M., Zkar S.O., *International journal of hydrogen energy*, **34**, 7223–7230 (2009)
58. Christensen N.E. and Seraphin B.O., *Solid State Communication*, **8**, 1221-1226 (1970)
59. Liu X., Xu H., Xia H., and Wang D., *Langmuir*, **28**, 13720–13726 (2012)
60. Yanase A. and Komiyama H., *Surface Science*, **264**, 147-156 (1992)
61. Shirtcliffe N., Nickel U. and Schneider S., *J. Col. Int. Sci.*, **211**, 122–129 (1999)
62. Lee S., Gu G. H., Suh J. S., *Chemical Physics Letters*, **511**, 121–125 (2011)
63. Zhang A., Fang Y., Shao H., *J. Col. Int. Sci.*, **298**, 769–772 (2006)
64. Zhang A., Fang Y., *Chemical Physics*, **332**, 284–288 (2007)
65. Shirtcliffe Neil, Nickel Ulrich and Siegfried Schneider, *J. Col. Int. Sci.*, **211**, 122–129 (1999)
66. Catherine J. Murphy and Nikhil R. Jana, *Adv. Mater.* **14(1)**, 80-82 (2002)
67. Zhi-Chuan Xu, Cheng-Min Shen, Cong-Wen Xiao, Tian-Zhong Yang, Huai-Ruo Zhang, Jian-Qi Li, Hu-Lin Li and Hong-Jun Gao, *Nanotechnology*, **18** 115608 (1-5) (2007)

68. Nikhil R. Jana, Latha Gearheart and Catherine J. Murphy, *Adv. Mater.*, **13(18)**, 1389-1393 (2001)
69. Hsiang-Yang Wu, Wan-Ling Huang, and Michael H. Huang, *Crystal Growth & Design*, **7(4)**, 831-835 (2007)
70. Jinxin Gao, Christopher M. Bender, and Catherine J. Murphy, *Langmuir*, **19**, 9065-9070 (2003)
71. Xiaohu Xia, Jie Zeng, Qiang Zhang, Christine H. Moran, and Younan Xia, *J. Phys. Chem. C*, **116 (41)**, 21647–21656 (2012)
72. Y. Ying Yu, S. Sing Chang, C. Liang Lee, and Chris Wang C. R., *J. Phys. Chem. B*, **101(34)**, 6661-6664 (1997)
73. Esumi K., Matsuhisa K., Torigoe K., *Langmuir*, **11**, 3285-3287 (1995)